Available online at www.sciencedirect.com
SCIENCE DIRECT®
Journal of Magnetic Resonance 167 (2004) 107–113
JMR Journal of Magnetic Resonance
www.elsevier.com/locate/jmr

Accurate relaxation parameters for large proteins

Aleksandras Gutmanas,[a] Luan Tu,[b] Vladislav Yu. Orekhov,[b] and Martin Billeter[a,*]

[a] *Biophysics Group, Department of Chemistry, Göteborg University, Box 462, 405 30 Göteborg, Sweden*
[b] *Swedish NMR Centre, Göteborg University, Box 465, 405 30 Göteborg, Sweden*

Received 20 October 2003; revised 1 December 2003

Abstract

The practical applicability, performance, and robustness of three-way decomposition (TWD) for the extraction of relaxation parameters are demonstrated for a large protein with 370 residues, the maltose binding protein. An ordinary set of seven relaxation-modulated ^{15}N HSQC spectra, recorded at another site, is systematically analyzed. For all 341 assigned backbone amide groups, including 21 pairs and one group of three overlapped peaks, T_1 decay values were determined. On isolated peaks, TWD extracts T_1 values with systematically lower error bounds compared to conventional tools, although for these simple cases the improvements remain limited. However, in the presence of spectral artifacts, the decrease in errors can become significant, demonstrating the higher robustness of TWD. For about half of the peaks in overlapped regions, the decomposition allowed separation of the signals, yielding significantly different T_1 values between overlapping signals. For the rest, similarity of the decay times for the two or three overlapping signals could be confirmed within usually low error bounds. The use of TWD thus leads to a significant increase in the number of accessible relaxation probes in large proteins. With a newly implemented graphical user interface, the application of TWD requires merely a peak list, and thus no additional effort compared to conventional approaches is needed.

Keywords: Dynamics; Maltose binding protein; MUNIN; NMR; Three-way decomposition

1. Introduction

Currently we witness an increasing interest in experimental observation of internal dynamics of proteins by NMR [1,2]. Novel approaches are being developed that increase the range of observable motions [3–6]. Measurements at various temperatures and magnetic fields allow thermodynamic characterizations of proteins by free energies, enthalpies, entropies, or heat capacities [7–10]. One of the major advantages of NMR for the study of internal dynamics, the ability to resolve individual residues, is currently extended from the routine application to ^{15}N–^{1}H moieties to relaxation measurements of various atom groups of the side chains, in particular methyl groups [11–13]. Usually, the basic experiment is a two-dimensional spectrum, e.g., a ^{15}N HSQC, and peak intensities are followed in a series of such experiments where a relaxation period is varied. Accuracy of the intensity measurements is often a limiting factor for the interpretation of the data in terms of dynamics. With larger proteins or with the use of CH_n moieties, overlap becomes an increasing problem [14]. Here we show that three-way decomposition [15] can provide an improvement in accuracy, in particular when considering overlapped peaks. A systematic analysis of the 370-residue long protein MBP (maltose binding protein [16]) was performed both by three-way decomposition (TWD) as implemented in the software MUNIN [17] and by a conventional procedure that is based on extracting the maximal intensity for each peak in each spectrum.

The fundamental model assumption of TWD is best described by the following expression:

$$\min\left[\sum_{ijk}\left|S_{ijk}-\sum_{m=1}^{M}a^m\cdot F1_i^m\cdot F2_j^m\cdot F3_k^m\right|^2+\lambda\sum_{m=1}^{M}(a^m)^2\right].$$

A 3D data set (e.g., a 3D spectrum or a set of 2D spectra) with data points S_{ijk} is to be optimally modeled by a sum of M components, i.e., the components should be determined such that the difference between the

* Corresponding author. Fax: +46-31-773-3910.
E-mail address: martin.billeter@bcbp.gu.se (M. Billeter).

1090-7807/$ - see front matter © 2003 Elsevier Inc. All rights reserved.
doi:10.1016/j.jmr.2003.12.002

experimental spectrum and the sum of components becomes minimal [17]. Each component m ($m = 1, 2, \ldots, M$) is a 3D entity that approximates a subset of the signals in the spectrum. It is in turn described by an amplitude a^m and a direct product of 3 one-dimensional vectors $F1^m$, $F2^m$, and $F3^m$. The one-dimensional vectors are referred to as shapes, and they resemble spectral cross-sections. The last sum in the above expression describes regularization according to Tikhonov [18]. By minimizing also the sum of squares of amplitudes a^m, one prevents that some components become much larger than others. The major benefits are faster convergence and avoidance of solutions with very similar components. Its weighting factor λ is called regularization parameter and, as shown previously [19], a value between 0.001 and 0.01 improves the convergence significantly. MUNIN, an implementation of TWD for NMR purposes, takes a spectrum S and an estimate M for the number of components as input and determines the amplitudes a^m and the vectors $F1^m$, $F2^m$, and $F3^m$ such that the above expression becomes minimal. It has been introduced earlier for the analysis of various types of NMR data sets, and both the model and the optimization algorithm have been discussed [17–22]. The principal feasibility of the algorithm for extracting relaxation parameters from a set of ^{15}N HSQCs was previously demonstrated on a few residues of azurin [23]. Here, we show the practical applicability, performance, and robustness of the method by systematically analyzing a large protein with 370 residues, maltose binding protein (MBP), using data recorded in another lab and not with TWD in mind. Ease of use is also increased by a new program version with a graphical user interface, requiring merely spectra in Nmrpipe format [24] and a peak list.

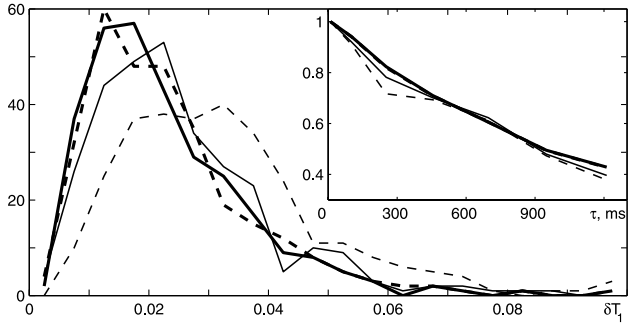

Fig. 1. Comparison of T_1 value evaluation from isolated peaks by MUNIN and a conventional method. Main panel: histograms of the distributions of relative errors in T_1 values of 296 isolated peaks. Results are shown for the conventional method (thin lines) and MUNIN (thick lines) applied to the data processed with linear prediction (dashed lines) and without it (solid lines). The relative error size is on the horizontal axis. Inset: example of relaxation profiles from the two methods. For this peak, a large error reduction from 9 to 5% of the T_1 value from the conventional method from the avoidance of linear prediction. Line styles are the same as in the main panel (note that the two thick lines almost coincide). The curves are scaled to set their maxima equal to unity. The input data comes from a ^{15}N T_1 relaxation data set consisting of seven spectra with 576×280 complex points each and relaxation times between 10.1 and 1211.5 ms. The data were recorded on a 600 MHz Varian Inova system at the University of Toronto. The spectra were processed by the Nmrpipe software [24] with or without doubling of the ^{15}N dimension by linear prediction, yielding Fourier transformed planes with 2048×1024 real points. The locations of peak maxima were restricted to small rectangles with a typical size of 8 data points (0.059 ppm) in the ^1H_N and 10 points (0.26 ppm) in the ^{15}N dimension. For non-overlapped peaks the same rectangles were also used to define the input for MUNIN. Least squares fits of single exponents, using a routine from the DASHA package [30], were applied to the intensities determined by both the MUNIN-based and the conventional approach, yielding relaxation times and their errors. The uncertainties in T_1 values were in all cases carefully estimated by 500 simulation runs of the Monte Carlo method [25] implemented in the above package.

2. Results and discussion

The 370 residues of MBP include 21 prolines and 8 residues including the N-terminus with unassigned backbone amide groups. Of the 341 assigned peaks, 296 were isolated in the spectrum, while 21 peak pairs exhibited significant overlap; there was also a group of 3 overlapped peaks. We considered two peaks being overlapped if the chemical shift difference was smaller than 0.04 ppm in the ^1H_N and 0.1 ppm in the ^{15}N dimension (see the caption to Fig. 1 for details of spectra acquisition and processing).

In a first step all 296 isolated and assigned peaks in the first spectrum were identified, and each peak was surrounded by a rectangle. This step is required for both MUNIN and a conventional approach used for comparison, which is based on the evaluation of the maximum of a peak in each spectrum (see the caption to Fig. 1 for details of the approaches). All seven spectra were then submitted together with the definitions of rectangular regions to both methods. A comparison of the two results shows primarily that the obtained T_1 values from MUNIN and the conventional method are consistent. For 286 of the 296 residues with isolated peaks in the ^{15}N HSQC the difference between the T_1 values from the two methods is smaller than the sum of the two corresponding errors. However, some of the remaining 10 cases exhibited significant differences as well as sizeable sums of errors. The source of these inconsistencies is indicated by looking at the distribution of error sizes among all 296 residues obtained from the two methods. Fig. 1 (main panel) plots the number of occurrences of errors versus their relative sizes (since all T_1 values are of similar order, the use of absolute errors would yield a similar distribution). The distribution of errors obtained by MUNIN (thick dashed line) is clearly shifted to smaller error values when compared to the corresponding curve for the conventional method (thin dashed line). This can be statistically proven by the

one-sided Kolmogorov–Smirnov test [25] implemented in MATLAB (The MathWorks). This test addresses the question whether two data sets, with elements that do not adopt predefined discrete values, are drawn from the same or from different (unknown) distributions. In our case it indicates different distributions at a significance level of more than 99%. Visual inspection of a number of cases with sizably larger errors from the conventional method revealed unwanted artifacts that are caused by the spectral processing. The inset of Fig. 1 displays for a selected peak (residue 62) the normalized intensities resulting from MUNIN and the conventional approach (thick and thin dashed lines, respectively). Clearly, the intensities from the latter method, in particular for the third spectrum, do not fall on a single exponential curve.

It is known that such artifacts, which did not show up in a consistent way but rather affected only a few peaks in only a few spectra, could be caused by the use of linear prediction [26,27]. Indeed, reprocessing the spectra without linear prediction and subsequent analysis by the conventional method significantly improved the result (thin solid line in Fig. 1, both panels) so that the distribution became more similar to the one from MUNIN. Analysis of the newly processed data by MUNIN yielded little change with respect to the original data (thick solid lines). Still, based on the Kolmogorov–Smirnov test, the error distribution for MUNIN remained better than for the conventional method on a 95% significance level. The 10 inconsistencies mentioned above, with differences of the T_1 values between the two methods exceeding the sum of errors, all disappeared when linear prediction was omitted. This was due to new T_1 values from the conventional method differing by up to three times the fitting error, while the new T_1 values from MUNIN changed only by a fraction of the fitting error. Changes of the results from the conventional

Table 1
Overlapped peaks with significant separation of the T_1 values

Residue	δ_N[a]	δ_H[a]	T_1 (M)[b]	T_1 (C)[b]	ΔT_1 (M)[c]	ΔT_1 (C)[c]
4[d]	123.2	8.41	806 ± 31	908 ± 31	644	170
350[d]	123.3	8.39	1450 ± 37	1078 ± 33		
269	118.8	8.09	1493 ± 37	1455 ± 43	179	113
328	118.8	8.06	1314 ± 32	1342 ± 29		
11	122.9	8.66	1269 ± 42	1275 ± 33	163	105
168	122.9	8.62	1432 ± 20	1380 ± 23		
46	120.9	8.05	1336 ± 24	1323 ± 29	127	100
363	120.8	8.05	1463 ± 47	1423 ± 15		
27	120.9	7.96	1497 ± 35	1473 ± 37	112	92
367	121.0	7.93	1385 ± 29	1381 ± 22		
283	117.1	7.07	1305 ± 58	1385 ± 8	196	35
310	117.2	7.07	1501 ± 89	1420 ± 31		
95[d]	115.6	7.36	1337 ± 17	1403 ± 32	193	37
297[d]	115.5	7.36	1530 ± 57	1440 ± 43		
280	120.7	8.21	1372 ± 28	1313 ± 30	184	64
303	120.7	8.18	1188 ± 70	1249 ± 51		
55	119.9	7.45	1177 ± 19	1219 ± 15	180	32
195	120.0	7.42	1357 ± 39	1251 ± 18		
151	124.9	7.24	1433 ± 37	1399 ± 18	109	31
338	124.9	7.22	1324 ± 57	1368 ± 28		
357	122.1	8.61	1379 ± 43	1392 ± 31	101	46
360	122.2	8.62	1480 ± 25	1438 ± 7		

[a] Shifts from an independent assignment, in ppm.
[b] T_1 values and their fitting errors obtained from MUNIN (M) and a conventional procedure (C), in ms.
[c] Difference between T_1 values in each pair for the two approaches, in ms.
[d] Examples for these pairs are presented in Figs. 2 and 3, respectively.

method gave rise to two new situations where the difference between the two methods exceeds the sum of errors, but both described low intensity shoulders of other strong peaks. Due to the results shown in Fig. 1, we decided to abandon our initial ambition to use the processed spectra exactly as they were provided to us, and rely for the remaining analysis exclusively on the spectra processed without linear prediction. The present analysis is not meant to address (well-known) questions about linear prediction [26,27], but we note that MUNIN proves to be more robust with respect to artifacts found in NMR spectra.

The next step involved the analysis of pairs of overlapped peaks. Two types of problems are expected in this situation. Firstly, the position of the maximum of each peak is falsified by the asymmetric contribution of intensity from the second peak, making it difficult to locate the measurement point by the conventional method. Secondly, the contributions from the overlapped peaks modify the measured intensities, yielding an averaging of the extracted peak intensities and thus of the resulting T_1 values. A straightforward calculation shows that these effects are not negligible. For two identical Lorentzian peaks separated by one line width in each dimension, the maxima are shifted towards each other by 20% of the line widths (along the ^{1}H and ^{15}N dimensions), and the contributions from the neighboring peaks reach 20% of the total intensity at the original and almost 30% at the new positions of the maxima. Since the latter effect causes the observed T_1 values in the pair to become more similar, we consider the size of the difference of T_1 values calculated for the two peaks of an overlapped pair an indication of the quality of the result. Our experience with TWD shows that the method hardly alters the difference in T_1 values, and in particular it does not increase it artificially.

Analysis of the 21 pairs of overlapped peaks, either by MUNIN using rectangles encompassing both peaks of a pair or by the conventional approach treating the peaks individually, yielded in 11 cases for at least one of the methods significant differences of the T_1 values (i.e., exceeding the sum of the corresponding errors). Table 1 shows that for all these pairs of residues MUNIN yielded a larger separation indicating more accurate values. For about half of the pairs, a significant difference of T_1 values is only obtained by TWD (lower half of Table 1). Figs. 2 and 3 show two examples of decomposition of pairs of overlapped peaks. For the pair of residues 4 and 350 (Fig. 2), a clean decomposition is obtained and a large difference in T_1 values is observed. The residue pair 95 and 297 (Fig. 3) represents a difficult case due to strong overlap, a smaller difference in T_1 values, which is

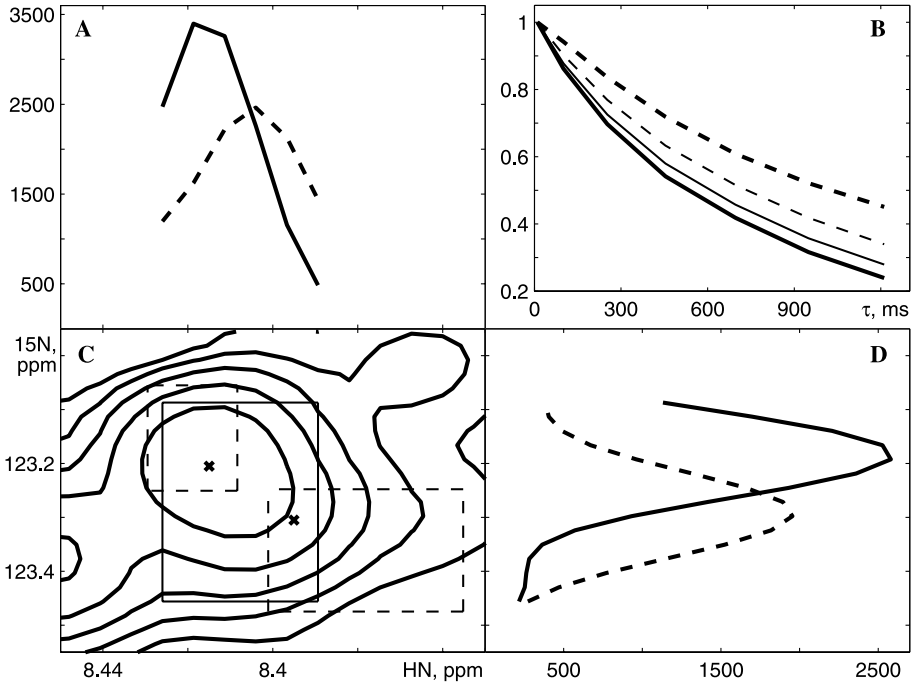

Fig. 2. Example of MUNIN decomposition of overlapped peaks corresponding to residues 4 and 350 (first pair in Table 1). (A) and (D) Shapes in frequency dimensions resulting from MUNIN decomposition; solid and dashed lines correspond to peaks 4 and 350, respectively. The intensity units are arbitrary, and all shapes are multiplied by the square root of the component amplitudes. (B) Peak relaxation profiles resulting from MUNIN (thick lines) and the conventional method (thin lines). Dashed and solid lines correspond to the same peaks as in (A) and (D). The curves are scaled to set their maxima equal to unity. (C) Contour plot of the peaks in the first HSQC-like plane; the solid rectangle shows the data submitted to MUNIN and the dashed ones indicate the regions submitted to the conventional procedure; the crosses indicate the positions of the peaks according to the assignment.

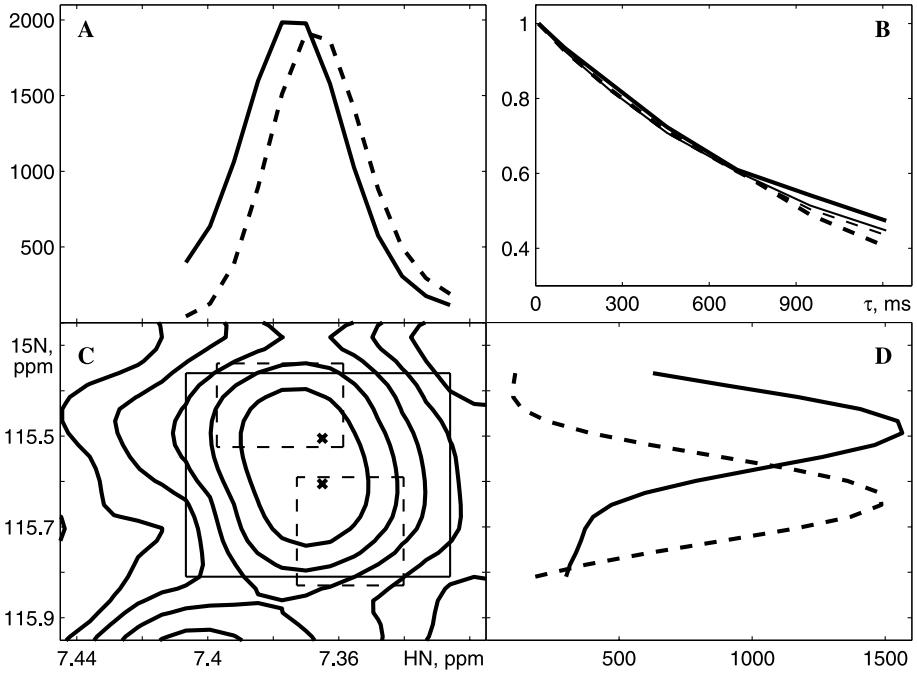

Fig. 3. Example of MUNIN decomposition of overlapped peaks corresponding to peaks 95 and 297 (pair seven in Table 1). Panel arrangement, axes and line types are analogous to Fig. 2. Solid lines in (A, B, and, D) correspond to residue 297 and dashed to residue 95.

only observable by the MUNIN approach, and a poorer fit to the anticipated exponential curve, mainly caused by the measurements at 696 and 1211 ms. Nonetheless, omitting measurements for any one delay time from the fit of the MUNIN data still retains a difference in T_1 values for the two components that exceeds their sum of errors. For example, omitting the measurements for 1211 ms yields a ΔT_1 (M) of 122 ms with a sum of errors of 73 ms. In both examples, the shapes describing the frequency dimensions of the peaks (panels A and D) are symmetric and "peak-like." The relaxation profiles from the conventional procedure are averaged compared to the MUNIN results. Both the decomposition into peaks with expected line-shapes and the higher separation of the T_1 values indicate the increased reliability of the TWD approach. For three peaks of these two pairs, the change in the T_1 value when switching from the conventional to the MUNIN approach exceeds the corresponding sum of errors; the exception is peak 297 due to relatively large errors (Table 1). The higher reliability when using TWD for the peak pairs of Table 1 increases also the confidence of those pairs of overlapped peaks where no difference in relaxation times could be determined. Summarizing, the MUNIN analysis of overlapped peak pairs may provide up to 42 additional probes for the characterization of backbone relaxation in MBP.

We also analyzed the remaining group of three overlapped peaks. It is however difficult to draw any conclusions from this result, as two of the three peaks overlapped exactly according to the assignment. Decomposition of the data into three components yielded reasonable and plausible shapes in the two frequency dimensions. However, the resulting T_1 values were similar within the corresponding errors. Using only two components for decomposition also provided undistorted shapes. Such a situation may be explained if two peaks are strongly overlapped and have very similar T_1 values, so that TWD may successfully describe the intensities by using only one component for both peaks. Information about the presence of a third peak thus has to come from other sources, e.g., the assignment. Irrespective of whether two or three components were proposed to MUNIN, the calculations provided peak definitions with regular shapes and a common relaxation time.

Use of Tikhonov regularization [18] was necessary when decomposing overlapped peaks because the variation among the different relaxation times was seldom more than 30% of a typical T_1 value. Such similarity, combined with a significant overlap in the frequency dimensions, may easily cause poor convergence. For some examples of Table 1, the use of a conventional approach based simply on intensity measurements may not be appropriate and one may instead consider the use of more sophisticated fitting routines, such as the "nlinLS" routine in Nmrpipe [24]. In contrast to MUNIN, these routines require as an input "estimates for all model parameters such as peak positions and line width" (Nmrpipe reference manual). Moreover, they demand the choice of a line shape model such as Gaussian or Lorentzian lines, which is known to be

problematic for decomposition of spectral regions [28,29]. Due to the number of parameter estimations requested it was not feasible to perform an objective comparison between such routines and MUNIN.

A new version of MUNIN, equipped with a graphical user interface, was designed for the analysis of relaxation data (available from the authors). It merely requires an input of processed spectra and a peak list. Rectangles defining the extensions of the peaks may be added to the peak list, but they can also be created in a semi-automated way while analyzing overlap situations interactively within the program.

3. Conclusion

The present systematic study, performed on a standard data set for a large protein, indicates that TWD extracts relaxation data from a set of HSQC-like spectra more reliably than other routinely used tools. Although the above observations with regard to linear prediction do not represent a systematic analysis of the influence of spectral artifacts, they do indicate that TWD presents a more robust method for the evaluation of relaxation data. A likely explanation is the necessity for TWD to describe corresponding peaks in all spectra by a single shape for each of the two dimensions. However, in the context of relaxation data, the major advantage of TWD is its ability to decompose overlapped signals without additional assumptions on line shapes or peak positions, and thus to significantly increase the number of accessible relaxation probes. It appears advisable to use interleaved recording of the set of spectra to minimize the effect of instrument or temperature instability and thus provide data that more closely fit the basic model assumption of TWD; this mode of data acquisition was however not used in the present application.

Acknowledgments

The authors would like to thank Drs. Vitaly Tugarinov and Lewis E. Kay from the University of Toronto for generously providing the relaxation spectra on MBP. The project was supported by the Swedish NMR Centre and by Grants 621-2001-3095 and 621-2001-3014 from the Swedish Research Council.

References

[1] D.M. Korzhnev, M. Billeter, A.S. Arseniev, V.Y. Orekhov, NMR studies of Brownian tumbling and internal motions in proteins, Prog. Nucl. Magn. Res. Spectrosc. 38 (2001) 197–266.

[2] M. Akke, NMR methods for characterizing microsecond to millisecond dynamics in recognition and catalysis, Curr. Opin. Struct. Biol. 12 (2002) 642–647.

[3] R. Ishima, D.A. Torchia, Estimating the time scale of chemical exchange of proteins from measurements of transverse relaxation rates in solution, J. Biomol. NMR 14 (1999) 369–372.

[4] O. Millet, J.P. Loria, C.D. Kroenke, M. Pons, A.G. Palmer, The static magnetic field dependence of chemical exchange linebroadening defines the NMR chemical shift time scale, J. Am. Chem. Soc. 122 (2000) 2867–2877.

[5] M. Tollinger, N.R. Skrynnikov, F.A. Mulder, J.D. Forman-Kay, L.E. Kay, Slow dynamics in folded and unfolded states of an SH3 domain, J. Am. Chem. Soc. 123 (2001) 11341–11352.

[6] A.G. Palmer 3rd, C.D. Kroenke, J.P. Loria, Nuclear magnetic resonance methods for quantifying microsecond-to-millisecond motions in biological macromolecules, Methods Enzymol. 339 (2001) 204–238.

[7] D. Yang, Y.K. Mok, J.D. Forman-Kay, N.A. Farrow, L.E. Kay, Contributions to protein entropy and heat capacity from bond vector motions measured by NMR spin relaxation, J. Mol. Biol. 272 (1997) 790–804.

[8] F.A. Mulder, B. Hon, A. Mittermaier, F.W. Dahlquist, L.E. Kay, Slow internal dynamics in proteins: application of NMR relaxation dispersion spectroscopy to methyl groups in a cavity mutant of T4 lysozyme, J. Am. Chem. Soc. 124 (2002) 1443–1451.

[9] E.Z. Eisenmesser, D.A. Bosco, M. Akke, D. Kern, Enzyme dynamics during catalysis, Science 295 (2002) 1520–1523.

[10] D.M. Korzhnev, B.G. Karlsson, V.Y. Orekhov, M. Billeter, NMR detection of multiple transitions to low-populated states in azurin, Protein Sci. 12 (2003) 56–65.

[11] F.A. Mulder, A. Mittermaier, B. Hon, F.W. Dahlquist, L.E. Kay, Studying excited states of proteins by NMR spectroscopy, Nat. Struct. Biol. 8 (2001) 932–935.

[12] F.A. Mulder, N.R. Skrynnikov, B. Hon, F.W. Dahlquist, L.E. Kay, Measurement of slow (μs–ms) time scale dynamics in protein side chains by ^{15}N relaxation dispersion NMR spectroscopy: application to Asn and Gln residues in a cavity mutant of T4 lysozyme, J. Am. Chem. Soc. 123 (2001) 967–975.

[13] N.R. Skrynnikov, F.A. Mulder, B. Hon, F.W. Dahlquist, L.E. Kay, Probing slow time scale dynamics at methyl-containing side chains in proteins by relaxation dispersion NMR measurements: application to methionine residues in a cavity mutant of T4 lysozyme, J. Am. Chem. Soc. 123 (2001) 4556–4566.

[14] V. Tugarinov, L.E. Kay, Side chain assignments of Ile delta 1 methyl groups in high molecular weight proteins: an application to a 46 ns tumbling molecule, J. Am. Chem. Soc. 125 (2003) 5701–5706.

[15] R. Bro, PARAFAC. Tutorial and applications, Chemometr. Intell. Lab. 38 (1997) 149–171.

[16] K.H. Gardner, X.C. Zhang, K. Gehring, L.E. Kay, Solution NMR studies of a 42 kDa *Escherichia coli* maltose binding protein beta-cyclodextrin complex: chemical shift assignments and analysis, J. Am. Chem. Soc. 120 (1998) 11738–11748.

[17] V.Y. Orekhov, I.V. Ibraghimov, M. Billeter, MUNIN: a new approach to multi-dimensional NMR spectra interpretation, J. Biomol. NMR 20 (2001) 49–60.

[18] I.V. Ibraghimov, Application of the three-way decomposition for matrix compression, Numer. Linear Algebra Appl. 9 (2002) 551–565.

[19] V.Y. Orekhov, I.V. Ibraghimov, M. Billeter, Optimizing resolution in multidimensional NMR by three-way decomposition, J. Biomol. NMR 27 (2003) 165–173.

[20] C.S. Damberg, V.Y. Orekhov, M. Billeter, Automated analysis of large sets of heteronuclear correlation spectra in NMR-based drug discovery, J. Med. Chem. 45 (2002) 5649–5654.

[21] A. Gutmanas, P. Jarvoll, V.Y. Orekhov, M. Billeter, Three-way decomposition of a complete 3D (15)N-NOESY-HSQC, J. Biomol. NMR 24 (2002) 191–201.

[22] M. Billeter, V.Y. Orekhov, in: P.M.A. Sloot, D. Abramson, A.V. Bogdanov, J.J. Dongarra, A.Y. Zomaya, Y.E. Gorbachev (Eds.), Computational Science—ICCS2003, Springer, St. Petersburg, 2003, pp. 15–24.

[23] D.M. Korzhnev, I.V. Ibraghimov, M. Billeter, V.Y. Orekhov, MUNIN: application of three-way decomposition to the analysis of heteronuclear NMR relaxation data, J. Biomol. NMR 21 (2001) 263–268.
[24] F. Delaglio, S. Grzesiek, G.W. Vuister, G. Zhu, J. Pfeifer, A. Bax, Nmrpipe—a multidimensional spectral processing system based on unix pipes, J. Biomol. NMR 6 (1995) 277–293.
[25] W.H. Press, S.A. Teukolsky, W.T. Vetterling, B.P. Flannery, Numerical Recipes in C, second ed., Cambridge University Press, Cambridge, 1992.
[26] P. Koehl, Linear prediction spectral analysis of NMR data, Prog. Nucl. Magn. Res. Spectrosc. 34 (1999) 257–299.
[27] A.S. Stern, K.B. Li, J.C. Hoch, Modern spectrum analysis in multidimensional NMR spectroscopy: comparison of linear-prediction extrapolation and maximum-entropy reconstruction, J. Am. Chem. Soc. 124 (2002) 1982–1993.
[28] W. Denk, R. Baumann, G. Wagner, Quantitative-evaluation of cross-peak intensities by projection of two-dimensional noe spectra on a linear-space spanned by a set of reference resonance lines, J. Magn. Reson. 67 (1986) 386–390.
[29] R. Koradi, M. Billeter, M. Engeli, P. Güntert, K. Wüthrich, Automated peak picking and peak integration in macromolecular NMR spectra using AUTOPSY, J. Magn. Reson. 135 (1998) 288–297.
[30] V.Y. Orekhov, D.E. Nolde, A.P. Golovanov, D.M. Korzhnev, A.S. Arseniev, Processing of heteronuclear NMR relaxation data with the new software DASHA, Appl. Magn. Reson. 9 (1995) 581–588.